

First Principles Calculation of Anomalous Hall Conductivity in Ferromagnetic bcc Fe

Yugui Yao^{1,2,3}, L. Kleinman¹, A. H. MacDonald¹, Jairo Sinova^{4,1},T. Jungwirth^{5,1}, Ding-sheng Wang³, Engle Wang^{2,3}, Qian Niu¹¹Department of Physics, University of Texas, Austin, Texas 78712²International Center for Quantum Structure, Chinese Academy of Sciences, Beijing 100080, China³Institute of Physics, Chinese Academy of Sciences, Beijing 100080, China⁴Department of Physics, Texas A & M University, College Station, TX 77843-4242 and⁵Institute of Physics ASCR, Cukrovarnicka 10, 162 53 Praha 6, Czech Republic

(Dated: April 14, 2024)

We perform a first principles calculation of the anomalous Hall effect in ferromagnetic bcc Fe. Our theory identifies an intrinsic contribution to the anomalous Hall conductivity and relates it to the k-space Berry phase of occupied Bloch states. The theory is able to account for both dc and magneto-optical Hall conductivities with no adjustable parameters.

PACS numbers: 75.47.-m, 71.15.-m, 72.15.Eb, 78.20.Ls

In many ferromagnets the Hall resistivity, ρ_H , exhibits an anomalous contribution proportional to the magnetization of the material, in addition to the ordinary contribution proportional to the applied magnetic field, $\rho_H = R_0 B + R_s 4 M$ [1, 2, 3]. The anomalous Hall effect (AHE) has played an important role in the investigation and characterization of itinerant electron ferromagnets because R_s is usually at least one order of magnitude larger than the ordinary constant R_0 . Although the effect has been recognized for more than a century [2] it is still somewhat poorly understood, a circumstance reflected by the controversial and sometimes confusing literature on the subject. Previous theoretical work has failed to explain the magnitude of the observed effect even in well understood materials like Fe [4].

Karplus and Luttinger [5] pioneered the theoretical investigation of this effect, by showing how spin-orbit coupling in Bloch bands can give rise to an anomalous Hall conductivity (AHC) in ferromagnetic crystals. Their conclusion was questioned by Smith [6], who argued that R_s must vanish in a periodic lattice. Smith proposed an alternative mechanism, skew scattering, in which spin-orbit coupling causes spin polarized electrons to be scattered preferentially to one side by impurities. The skew scattering mechanism predicts an anomalous Hall resistivity linearly proportional to the longitudinal resistivity; this is in accord with experiment in some cases, but an approximately quadratic proportionality is more common. Later, Berger [7] proposed yet another mechanism, the side jump, in which the trajectories of scattered electrons shift to one side at impurity sites because of spin-orbit coupling. The side jump mechanism does predict a quadratic dependence of the AHC on the longitudinal resistivity. However, because of inevitable difficulties in modeling impurity scattering in real materials, it has not been possible to compare quantitatively with experiment. It appears to us that the AHE has generally been regarded as an extrinsic effect due solely to impurity scattering, even though this notion has never been critically

tested, and that the intrinsic contribution initially proposed by Karplus and Luttinger has been discounted.

Several years ago, the scattering free contribution of Karplus and Luttinger was rederived in a semiclassical framework of wavepacket motion in Bloch bands by taking into account Berry phase effects [8, 9]. According to this work, the AHC in the scattering free limit is a sum of Berry curvatures (see eqs. (2) and (6) below) of the occupied Bloch states [10]. Recently, Jungwirth et al. [11, 12] applied this picture of the AHE to (III,Mn)V ferromagnetic semiconductors and found very good agreement with experiment. (III,Mn)V ferromagnets are unusual, however, because they are strongly disordered and have extremely strong spin-orbit interactions. In this Letter, we report on an evaluation of the intrinsic AHC in a classic transition metal ferromagnet, bcc Fe. Our calculation is based on spin-density functional theory and the LAPW method. The close agreement between theory and experiment that we find leads us to conclude that the AHC in transition metal ferromagnets is intrinsic in origin, except possibly at low temperature in highly conductive samples.

We begin our discussion by briefly reviewing the semiclassical transport theory. By including the Berry phase correction to the group velocity [8, 9], one can derive the following equations of motion:

$$\begin{aligned} \dot{\mathbf{r}}_c &= \frac{1}{\hbar} \frac{\partial \epsilon_n(\mathbf{k})}{\partial \mathbf{k}} - \mathbf{v}_n(\mathbf{k}) \times \mathbf{v}_n(\mathbf{k}); \\ \dot{\mathbf{h}}_k &= e\mathbf{E} - e\mathbf{v}_c \times \mathbf{B}; \end{aligned} \quad (1)$$

where \mathbf{v}_n is the Berry curvature of the Bloch state defined by

$$\mathbf{v}_n(\mathbf{k}) = \text{Im} \langle \mathbf{r}_k | \nabla_{\mathbf{k}} u_{n\mathbf{k}} | \nabla_{\mathbf{k}} u_{n\mathbf{k}} \rangle; \quad (2)$$

with $u_{n\mathbf{k}}$ being the periodic part of the Bloch wave in the n th band. We will be interested in the case of $\mathbf{B} = 0$, for which $\epsilon_n(\mathbf{k})$ is just the band energy. The distribution function satisfies the Boltzmann equation with the

usual drift and scattering terms, and can be written as $f_n(\mathbf{k}) + f_n^s(\mathbf{k})$, where f_n is the equilibrium Fermi-Dirac distribution function and f_n^s is a shift proportional to the electric field and relaxation time. The electric current is given by the average of the velocity over the distribution function, yielding to first order in the electric field [13]

$$\frac{e^2}{h} E \sum_n \int \frac{d^3k}{(2\pi)^3} v_n(\mathbf{k}) f_n^s(\mathbf{k}) = \frac{e}{h} \sum_n \int \frac{d^3k}{(2\pi)^3} v_n(\mathbf{k}) \frac{\partial f_n}{\partial k} : \quad (3)$$

The same expressions can be derived from the Kubo linear-response-theory formula for the conductivity matrix. The first term is the anomalous Hall current originally derived by Karplus and Luttinger, but never previously evaluated. In the second term, apart from the longitudinal current, there can also be a Hall current in the presence of skew scattering because the distribution function can acquire a shift in the transverse direction. This skew scattering contribution to the Hall conductivity should be much smaller than, but crudely proportional to, the longitudinal conductivity and can be identified, when it is dominant, by the traditional test, i.e. $\sigma_{xy} / \sigma_{xx}$. It will have a larger relative importance when σ_{xx} is large, i.e. in pure-crystals at low temperatures.

We now discuss our scheme for calculating the Berry curvature and the AHC. For a cubic material with magnetization aligned along [001], only the z-component $\Omega_n^z(\mathbf{k}) \neq 0$. In our calculation, we find it convenient to use a different but equivalent expression for the Berry curvature that arises naturally from the Kubo formula derivation [14],

$$\Omega_n^z(\mathbf{k}) = \sum_{n' \neq n} \frac{2 \text{Im} \langle n | \hat{v}_x | n' \rangle \langle n' | \hat{v}_y | n \rangle}{(E_n - E_{n'})^2}; \quad (4)$$

where $E_n = \hbar v_n$; and \hat{v} 's are velocity operators. In the relativistic formulation, the $|n\rangle$'s are four-component Bloch wave functions, and $\mathbf{v} = c \begin{pmatrix} 0 & \boldsymbol{\sigma} \\ \boldsymbol{\sigma} & 0 \end{pmatrix}$, with $\boldsymbol{\sigma}$ being the Pauli matrix and c the speed of light. It will also be instructive to introduce the sum (for each \mathbf{k}) of Berry curvatures over the occupied bands:

$$\Omega^z(\mathbf{k}) = \sum_n f_n \Omega_n^z(\mathbf{k}); \quad (5)$$

Then the intrinsic AHC is an integration over the Brillouin zone (BZ):

$$\sigma_{xy} = \frac{e^2}{h} \int_{\text{BZ}} \frac{d^3k}{(2\pi)^3} \Omega^z(\mathbf{k}); \quad (6)$$

The recent development of highly accurate ab initio electronic structure calculation methods enables us to complete the work of Karplus and Luttinger by evaluating their intrinsic Hall conductivity and comparing

it with experiment. We employ the full-potential linearized augmented plane-wave method [15] with the generalized gradient approximation (GGA) for the exchange-correlation potential [16]. Fully relativistic band calculations were performed using the program package WIEN2K [17]. A converged ground state with magnetization in the [001] direction was obtained using 20,000 \mathbf{k} points in the first Brillouin zone and $K_{\text{max}} R_{\text{MT}} = 10$, where R_{MT} represents the muffin-tin radius and K_{max} the maximum size of the reciprocal-lattice vectors. In this calculation, wavefunctions and potentials inside the atomic sphere are expanded in spherical harmonics $Y_{lm}(\theta, \phi)$ up to $l = 10$ and 4, respectively, and 3s and 3p semi-core local orbitals are included in the basis set. The calculations were performed using the experimental lattice constant of 2.87 Å. The spin-magnetron number was found to be 2.226, compared to the experimental value of 2.12 as deduced from measurements of the magnetization [18] and of the g (≈ 2.09) factors. The calculated energy bands are shown in Fig. 1, and are very similar to those obtained in Ref. [19]. If the spin-orbit interaction is parameterized as $\lambda \mathbf{L} \cdot \mathbf{S}$, its strength is found to be approximately 5.1 mRy from the band splitting near the H point and the Fermi energy.

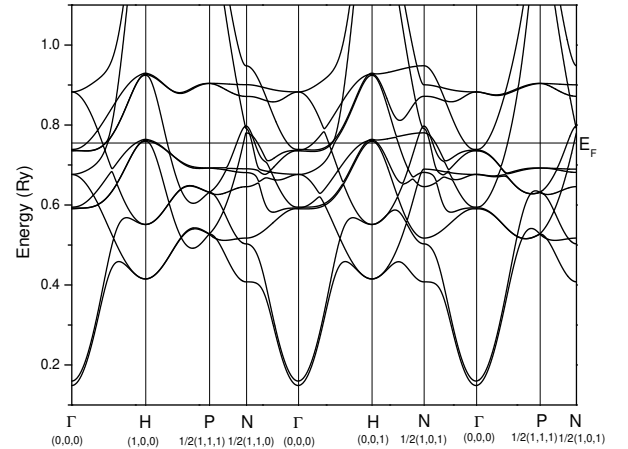


FIG. 1: Band structure of iron along high symmetry lines in the Brillouin zone. The magnetization direction is along [001].

After obtaining the self-consistent potential with 20,000 \mathbf{k} points, we calculated the Berry curvature with several larger sets of \mathbf{k} -points in order to achieve the convergence for σ_{xy} shown in Fig. 2. The Monkhorst-Pack special-point method [20] was used for the integration in Eq.(6). To go beyond 2,000,000 points, we adopted a method of adaptive mesh refinement, i.e., when $\Omega^z(\mathbf{k})$ is large at a certain \mathbf{k} point, we construct a finer mesh by adding 26 additional points around it. This procedure yields a converged value of $\sigma_{xy} = 751 (\text{cm})^2$ at zero temperature (using a step function for the Fermi-Dirac

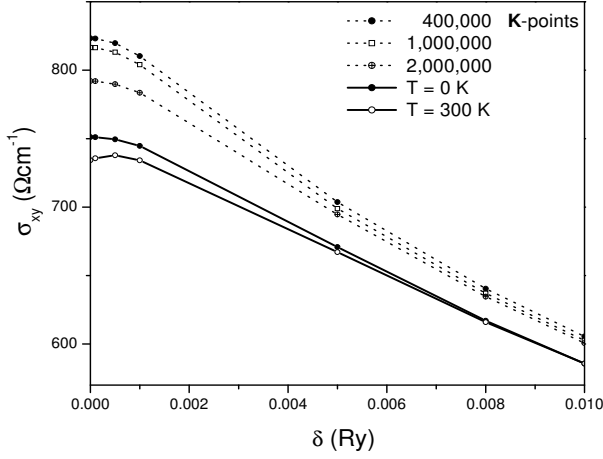


FIG. 2: Anomalous Hall effect vs. δ with different numbers of k points in full Brillouin zone. Here δ is introduced by adding δ^2 to the denominator in Eq.(4). The solid lines were obtained by an adaptive mesh refinement method.

distribution) and a slightly smaller value of $\sigma_{xy} = 734$ (Ωcm^{-1}) at room temperature (300 K). Our result is in fair agreement with the value 1032 (Ωcm^{-1}) extracted from Decker's data on iron whiskers [21] at room temperature.

The slow convergence is caused by the appearance of large contributions to Ω^z of opposite sign which occur in very small regions of k-space. Spin-orbit effects are small except when they mix states that would otherwise be degenerate or nearly degenerate, and even then, those mixed states will contribute nearly canceling contributions to Ω^z . Only when the Fermi surface lies in a spin-orbit induced gap is there a large contribution. This can be seen in Fig. 3 where the Berry curvature along lines in k-space is compared with energy bands near E_F and in Fig. 4 where it is compared with the intersection of the Fermi surface with the central (010) plane in the Brillouin zone.

In order to further understand the role of spin-orbit coupling in the AHE, we artificially varied the speed of light, thereby changing the spin-orbit coupling strength $\propto 1/c^2$. As shown in Fig. 5, σ_{xy} is linear in $1/c^2$ for small coupling, but not for large coupling. For iron, nonlinearities become significant for $1/c^2 > 1/2$, which means that the spin-orbit interaction in iron cannot be treated perturbatively.

So far we have discussed only the dc-AHE. It is straightforward to extend our calculation to the ac Hall case by using the Kubo formula [22] approach:

$$(\sigma)_{xy} = \frac{e^2}{h} \frac{1}{v_g} \frac{d^3 k}{(2\pi)^3} \sum_{n \neq n^0} \frac{X}{(f_{n,k} - f_{n^0,k})} \quad (7)$$

$$\frac{\text{Im} \langle n_k | \hat{v}_x | n^0_k \rangle \langle n^0_k | \hat{v}_y | n_k \rangle}{(f_{n^0} - f_n)^2 (1 + i)^2};$$

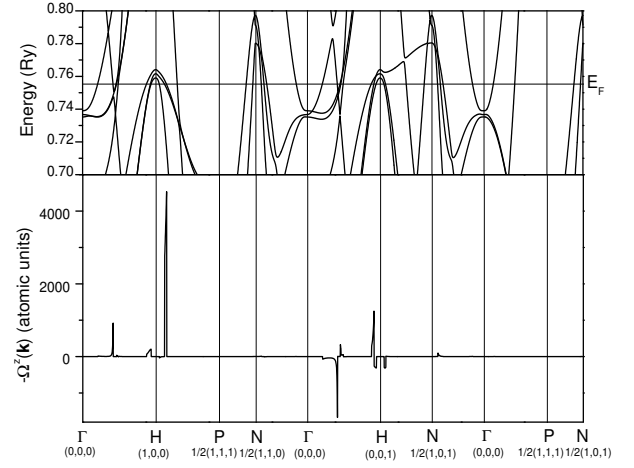


FIG. 3: Band structure near Fermi surface (upper figure) and Berry curvature $\Omega^z(k)$ (lower figure) along symmetry lines.

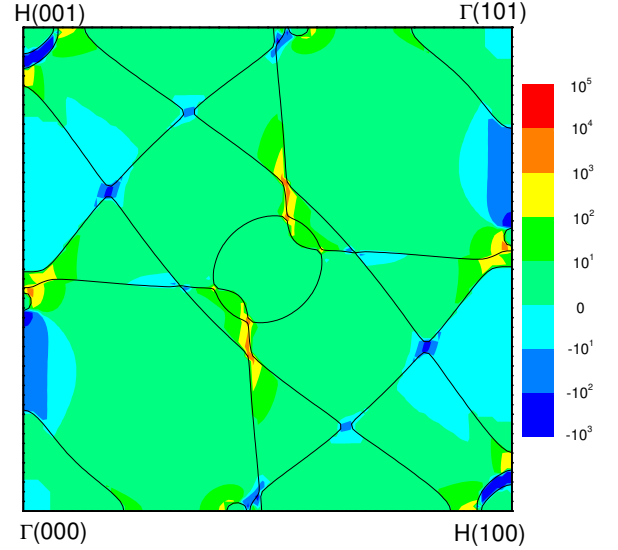


FIG. 4: (010) plane Fermi surface (solid lines) and Berry curvature $\Omega^z(k)$ (color map). Ω^z is in atomic units.

where δ is a positive infinitesimal. In the upper panel in Fig. 6, we show results for the imaginary part of σ_{xy} as a function of frequency that are in agreement with earlier calculations [23]. Experimental results [24] are in excellent agreement below 1.7 eV but become smaller at higher energies. In the lower panel of the figure, the real part of the Hall conductivity, obtained from the imaginary part by a Kramers-Kronig relation, is shown as a function of frequency. The dc limit result, $(\sigma = 0)_{xy} = 750.8$ (Ωcm^{-1}), is essentially identical to that obtained from Eq.(6). Despite the small discrepancy with theory in the dc limit, the experimental point [21] seems to agree rather well with the overall trend of the frequency de-

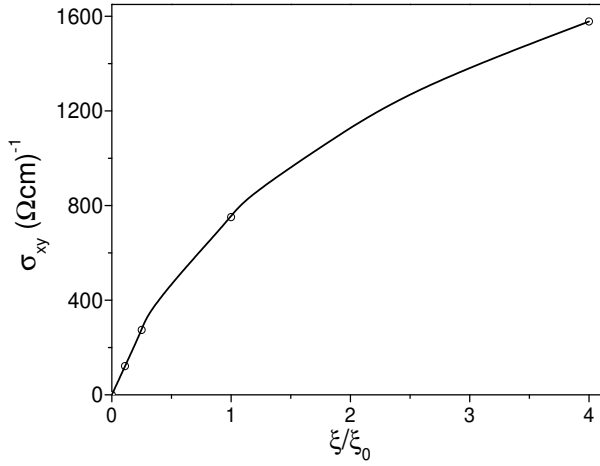


FIG. 5: Calculated anomalous Hall conductivity (open circles) vs. spin-orbit coupling, ξ_0 is spin-orbit coupling strength of iron. The line is a guide to the eye.

pendence of the calculated AHC.

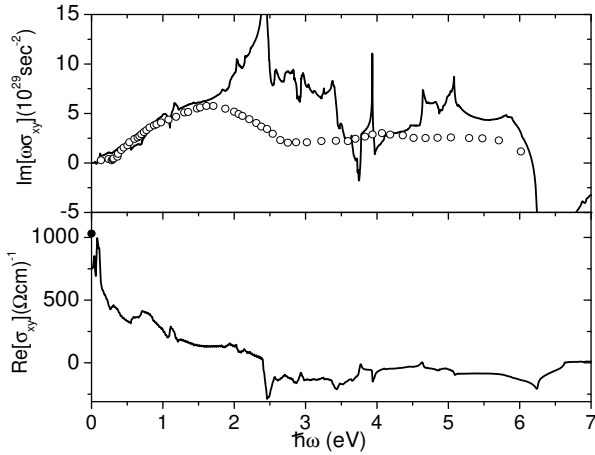


FIG. 6: Frequency dependence of the Hall conductivity at zero temperature. In the upper panel, the calculated imaginary part of σ_{xy} (solid curve) is compared with experimental results [Ref. (24)]. In the lower panel, the real part of σ_{xy} is shown together with the dc experiment value extracted from Ref. (21).

In conclusion we have shown that the AHC of bcc Fe, and presumably all other transition metal ferromagnets, is primarily intrinsic. (The only previous evaluation of the AHC of which we are aware [4] found that $\sigma_{xy} = 20.9 (\text{cm})^{-1}$ for Fe. The remaining discrepancy between theory and experiment is likely due to shortcomings of the GGA, neglect of scattering effects, and experimental uncertainties.

This work was supported by DOE/DE-FG03-02ER45958, and by the Welch Foundation. Y. Yao

also acknowledges financial support from the NSF of China (10134030, 60021403), the National Key Project for Basic Research (G2000067103), and the National Key Project for High-Tech (2002AA311150). L.K. was supported by NSF grant DMR-0073546. AHM and JS acknowledge helpful discussions with P. Bruno.

-
- [1] The Hall Effect and Its Application, edited by C.L. Chien and C.R. Westgate (Plenum, New York 1980).
 - [2] E.H. Hall, Phil. Mag. 10, 301 (1880); 12, 157 (1881)
 - [3] A.W. Smith and R.W. Sears, Phys. Rev. 34, 1466 (1929).
 - [4] Henri Leribaux, Phys. Rev. 150, 384 (1966).
 - [5] R. Karplus and J.M. Luttinger, Phys. Rev. 95, 1154 (1954).
 - [6] J. Smith, Physica 21, 877 (1955); J. Smith, Physica 24, 39 (1958).
 - [7] L. Berger, Phys. Rev. B 2, 4559 (1958).
 - [8] G. Sundaram and Q. Niu, Phys. Rev. B 59, 14915 (1999).
 - [9] M.P. Marder, Condensed Matter Physics (Wiley, New York, 1999), pp. 425-429.
 - [10] This is distinct from the Berry phase effect in real space discussed in J. Ye, et al., Phys. Rev. Lett. 83, 3737 (1999); Y. Taguchi, et al., Science 291, 2573 (2001); R. Shindou, et al., Phys. Rev. Lett. 87, 116801 (2001), where the AHE is related with non collinear spin-splitting effective fields produced by spin-lattice backgrounds.
 - [11] T. Jungwirth, Q. Niu, and A.H. MacDonald, Phys. Rev. Lett. 88, 207208 (2002).
 - [12] T. Jungwirth et al., Appl. Phys. Lett. 83, 320 (2003).
 - [13] J.M. Luttinger, Phys. Rev. 112, 739 (1958).
 - [14] D.J. Thouless, M. Kohmoto, M.P. Nightingale, and M. den Nijs, Phys. Rev. Lett. 49, 405 (1982).
 - [15] D.J. Singh Pseudopotentials and the LAPW Method (Kluwer Academic, Boston, 1994).
 - [16] J.P. Perdew, K. Burke, and M. Ernzerhof Phys. Rev. Lett. 78, 1396 (1997).
 - [17] P. Blaha, K. Schwarz, G.K.H. Madsen, D. Kvasnicka, and J. Luitz, WIEN 2K, An Augmented Plane Wave + Local Orbitals Program for Calculating Crystal Properties (Karlheinz Schwarz, Techn. Universität Wien, Austria), 2001. ISBN 3-951031-1-2.
 - [18] H. Danan, A. Herr, and A.J.P. Meyer, J. Appl. Phys. 39, 669 (1968).
 - [19] M. Singh, C.S. Wang, and J. Callaway, Phys. Rev. B 11, 287 (1975).
 - [20] H.J. Monkhorst and J.D. Park, Phys. Rev. B 13, 5188 (1976).
 - [21] P.N. Dheer, Phys. Rev. 156, 637 (1967). It was found that $R_{xy} = 43.1 \cdot 10^{-13} \text{ cm} = G$ at room temperature, $4 M_s = 21.6 \text{ kG}$, and $\chi_x = 9.5 \cdot 10^{-6} \text{ cm}$, yielding $\chi_y = 4 M_s R_{xy} / \chi_x = 1032 (\text{cm})^{-1}$.
 - [22] J. Sinova et al., Phys. Rev. B 67, 235203 (2003)
 - [23] N.M. Ainkar, D.A. Browne, and J. Callaway, Phys. Rev. B 53, 3692 (1996); G.Y. Guo and H. Ebert, Phys. Rev. B 51, 12633 (1995).
 - [24] G.S. Krinchik and V.A. Artem'ev, Zh. Eksp. Teor. Fiz. 53, 1901 (1967) [Sov. Phys.-JETP 26, 1080 (1967)].